

Effect of molding pressure on fabrication of low-crystalline calcite block

Xin Lin · Shigeki Matsuya · Masaharu Nakagawa ·
Yoshihiro Terada · Kunio Ishikawa

Received: 4 July 2006 / Accepted: 19 October 2006 / Published online: 3 July 2007
© Springer Science+Business Media, LLC 2007

Abstract We have reported that low-crystalline porous calcite block, which is useful as a bone substitute or a source material to prepare apatite-type bone fillers could be fabricated by exposing calcium hydroxide compact to carbon dioxide gas saturated with water vapor. In the present study, we investigated the effect of molding pressure on the transformation of calcium hydroxide into calcite and the mechanical strength of the carbonated compact. Transformation into calcite was almost completed within 72 h, however, a small amount of $\text{Ca}(\text{OH})_2$ still remained unreacted at higher molding pressure because of incomplete penetration of CO_2 gas into the interparticle space due to dense packing of $\text{Ca}(\text{OH})_2$ particles. On the other hand, high molding pressure resulted in an increase in diametral tensile strength (DTS) of the calcite compact formed. Critical porosity of the calcite block was calculated as approximately 68%.

Introduction

Calcium carbonate (CaCO_3) has been used as bone filler for the reconstruction of bone defects and as a source

material for bone fillers. Marine coral is made of aragonite-type calcium carbonate (>97%). The coral has been clinically used as bone substitute in dental, maxillo-facial, cranio-facial, and orthopedic surgeries for the reconstruction of bone defects [1–5]. The coral is also used as a source material to prepare apatite-type bone fillers. When the coral is hydrothermally treated in diammonium hydrogen phosphate solution, it transforms into apatitic mineral without changing its morphology. The bone filler is called coralline apatite and has been clinically used as a bone substitute in the United States [6–9]. However, the usage of the coral is limited due to its high cost and serious environmental problems. Moreover, the collected coral have to be cleaned to prevent inflammatory reaction caused by proteins and other elements present as impurities. Drawbacks of the coral mentioned above would be solved if calcium carbonate compact can be prepared artificially. Though the sintering of calcium carbonate powder results in calcium carbonate block, it would cause liberation of carbon dioxide and formation of calcium oxide above 650 °C. In addition, calcium carbonate with extremely high crystallinity is obtained even when low crystalline calcium carbonate powder is used. Unfortunately, formation of calcium oxide and high-crystalline calcium carbonate is not desirable with respect to tissue response and resorbability, when it is used as the bone substitute.

In our previous study [10], therefore, we proposed a fabrication method of pure, low-crystalline calcite compact with adequate and high mechanical strength calcium carbonate (calcite) compact by carbonation of calcium hydroxide ($\text{Ca}(\text{OH})_2$) compact in CO_2 stream saturated with water vapor. We found that development of DTS proceeded in two stage, which corresponded to rapid carbonation at the surface of the $\text{Ca}(\text{OH})_2$ particle and

X. Lin · M. Nakagawa · K. Ishikawa
Department of Biomaterials, Faculty of Dental Science,
Kyushu University, 3-1-1 Maidashi, Higashi-ku,
Fukuoka 812-8582, Japan

X. Lin · Y. Terada
Department of Fixed Prosthodontics, Faculty of Dental Science,
Kyushu University, Fukuoka, Japan

S. Matsuya (✉)
Section of Bioengineering, Department of Dental Engineering,
Fukuoka Dental College, Sawara-ku, Fukuoka 814-0193, Japan
e-mail: smatsuya@college.fdcnet.ac.jp

diffusion process through the calcite layer at the surface to complete carbonation. It was considered that DTS before and after carbonation depended on the molding pressure used.

In the present study, we investigated the formation process and measured DTS of calcite compact prepared by carbonation of $\text{Ca}(\text{OH})_2$ compact under wider range of molding pressure. The aim of this investigation was to clarify the effect of molding pressure on mechanical strength and to get more information about the fabrication process of calcite compact as a bone substitute and/or as a precursor for apatite block.

Materials and methods

Calcium hydroxide compact preparation

Commercially available calcium hydroxide ($\text{Ca}(\text{OH})_2$, Wako Chemicals, Tokyo, Japan) was used in this study. The $\text{Ca}(\text{OH})_2$ powder, 0.2 g, was placed in a stainless steel mold and pressed uniaxially with an oil pressure press machine (Riken Power, Riken Seiki, Japan) under 1–15 MPa pressure. Specimens prepared were 10 mm in diameter and 1–3 mm in height.

Carbonation of $\text{Ca}(\text{OH})_2$ compact

The prepared $\text{Ca}(\text{OH})_2$ compacts were placed in a reaction vessel saturated with water vapor at room temperature. Carbon dioxide gas was introduced in the vessel at a flow rate of 0.15–0.20 L/min and the $\text{Ca}(\text{OH})_2$ compacts were carbonated up to 72 h.

Mechanical testing

After the carbonation for the prescribed periods, mechanical strength of the specimens was evaluated in terms of diametral tensile strength (DTS). The specimens were crushed using a universal testing machine (IS5000, Shimadzu Co., Kyoto, Japan) at a cross-head speed of 1 mm/min after measuring the diameter and height of each specimen with a micrometer (156-101, Mitutoyo Co. Ltd., Kanagawa, Japan). The DTS values were averaged over at least eight specimens.

Microstructure

Morphology of the fractured surface of the specimen was characterized by means of a scanning electron microscope (SEM, JSM 5400LV, JEOL Co. Ltd., Tokyo, Japan) at 15 kV of accelerating voltage after gold sputter coating.

X-ray diffraction analysis

The specimens ground into fine powders were characterized by X-ray diffraction (XRD) analysis. The XRD patterns were recorded with a vertically mounted diffractometer system (RIGAKU RINT 2500V, Tokyo, Japan) using counter-monochromatized CuK_α radiation generated at 40 kV and 100 mA. The specimens were scanned from 3° to $60^\circ 2\theta$ (where θ is the Bragg angle) in a continuous mode at a scanning rate of $2^\circ/\text{min}$. Quantitative analysis was also done on the specimens during carbonation. Calibration curve for the quantitative analysis was made using separated diffraction peaks of $\text{Ca}(\text{OH})_2$ (0 0 1, $d = 4.905 \text{ \AA}$) and calcite (0 -2 2, $d = 2.095 \text{ \AA}$) respectively. Crystallite sizes, D of the calcite formed by carbonation for 72 h of $\text{Ca}(\text{OH})_2$ compact prepared at various molding pressures were calculated based on XRD analysis.

The following relation holds between half width (β) and crystallite size (D).

$$\beta \cdot \cos(\theta) = K\lambda/D$$

where θ and λ are Bragg angle and wave length of X-ray (CuK_α) used, respectively. After β was corrected for the instrumental broadening by using well crystallized α -quartz heated at $1,050^\circ\text{C}$, crystallite size was calculated based on the above equation.

Porosity measurement

For porosity measurement, the apparent density of specimen before and after carbonation was calculated from the specimen's weight and dimensions. The theoretical densities of pure calcium hydroxide (2.24 g/cm^3) and calcite (2.711 g/cm^3) were used for the calculation. As a small amount of calcium hydroxide still remained after the carbonation, its content was taken into account for the apparent density calculation. Relative density was calculated from a ratio of the apparent density to the theoretical density. The total porosity of specimen is then defined as

$$\text{Total porosity (\%)} = 100 (\%) - \text{Relative density (\%)}$$

Total porosity was averaged over at least five specimens.

Results

Figure 1 shows the X-ray diffraction patterns of calcium hydroxide compacts prepared at 2 MPa (A) and 15 MPa (B) and treated with CO_2 gas for up to 72 h. In each figure, a diffraction pattern of the sample (a) before carbonation

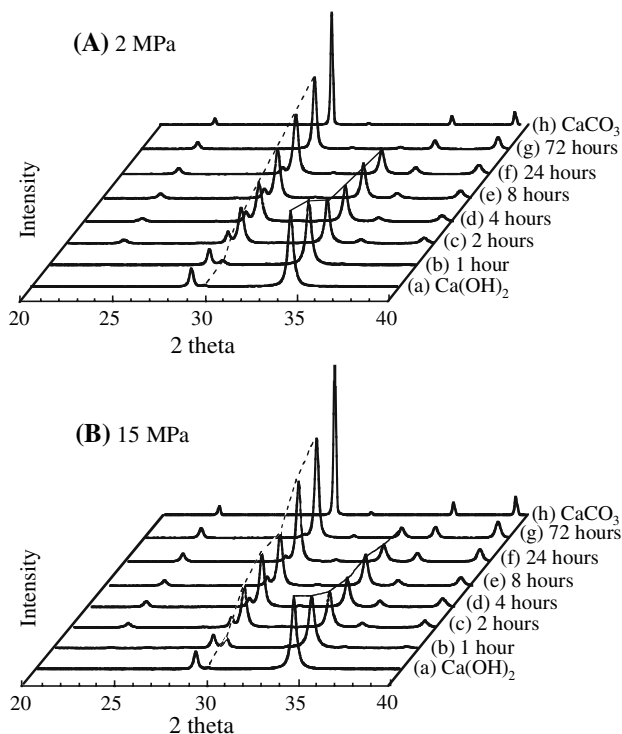


Fig. 1 X-ray diffraction patterns of calcium hydroxide compacts prepared at (A) 2 MPa and (B) 15 MPa treated with CO₂ gas for different time periods. In each figure, a diffraction pattern of the sample (a) before carbonation and (h) commercially contained calcite powder were also included for comparison. Specimens were treated with CO₂ gas for (b) 1 h, (c) 2 h, (d) 4 h, (e) 8 h, (f) 24 h, and (g) 72 h respectively

and (h) commercially contained calcite powder were also included for comparison. Specimens were treated with CO₂ gas for (b) 1 h, (c) 2 h, (d) 4 h, (e) 8 h, (f) 24 h, and (g) 72 h, respectively. As shown in this figure, the intensities of peaks attributed to calcium hydroxide, $2\theta = 28.7$ (0 -1 0) and $2\theta = 34.1$ (0 1 1), decreased gradually with time and meantime the intensities of peaks attributed to calcite, $2\theta = 29.4$ (0 -1 -4) and $2\theta = 36.0$ (1 1 0) appeared and their intensities increased with time in both cases. In the case of other molding pressures, the change in XRD patterns was quite similar though the data are not shown.

Table 1 Changes in the amount of calcite phase in the compacts with time at various molding pressures

Molding pressure (MPa)	CaCO ₃ (wt%)
1	99.8
2	97.7
3	97.2
5	98.5
7.5	92.8
10	90.1
15	86.3

Table 1 shows the amount of calcite formed after carbonation for 72 h at various molding pressure. As shown in this table, the amount of calcite varied between 86.3 wt% and 99.8 wt% and tended to decrease with increasing the molding pressure.

Table 2 summarizes crystallite size, D of the calcite formed by carbonation for 72 h of Ca(OH)₂ compact prepared at various molding pressures. Crystallite size of the initial calcium hydroxide powder was 30.2 nm. As can be seen in this table, crystallite size increased with molding pressure to reach 46.8 nm when compacted at 15 MPa. It should be noted that crystallite size of the calcite formed by the carbonation was much smaller than that of the commercial one (83.4 nm).

Figure 2 shows the SEM images of the fractured surfaces of calcium hydroxide compacts prepared at various molding pressures before carbonation (left column; (a)–(e)) and after carbonation for 72 h (right column; (f)–(i)), respectively. The original Ca(OH)₂ powder had particle size ranging from sub micron to several microns with an irregular shape. We found no remarkable differences in the surface structure before and after the carbonation for 72 h as shown in Fig. 2, nevertheless X-ray diffraction analysis showed that approximately 86–100 wt% of Ca(OH)₂ had transformed into calcite depending on the molding pressure.

Figure 3 shows the change in porosity of Ca(OH)₂ compact before and after carbonation for 72 h as a function of molding pressure. The porosity decreased with increase in molding pressure in spite of carbonation. Porosity after the carbonation was approximately 4% smaller than that before carbonation regardless of the molding pressure.

Figure 4 shows the change in DTS values of Ca(OH)₂ compacts prepared at various molding pressures as a function of carbonation time. Irrespective of the molding pressure, DTS values rapidly increased with time within

Table 2 Comparisons of crystallite size, D for each compact formed by carbonation for 72 h of Ca(OH)₂ compact prepared at various molding pressures

Molding pressure (MPa)	Crystallite size (nm)
Initial calcium hydroxide powder	30.2
1	35.5
2	36.9
3	35.2
5	35.3
7.5	42.3
10	45.1
15	46.8
commercial calcite powder	83.4

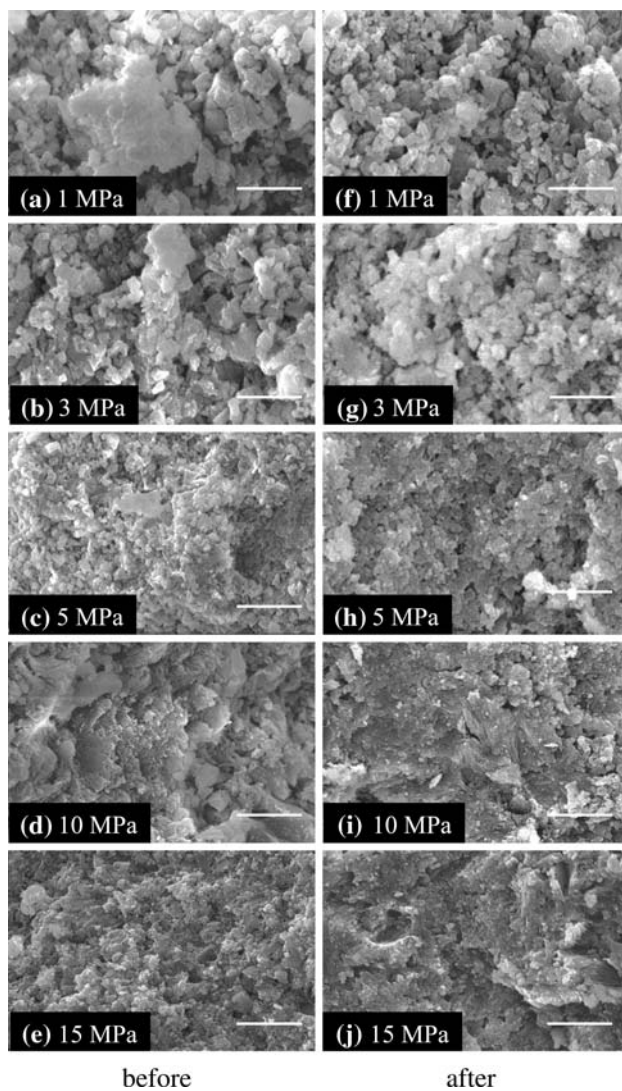


Fig. 2 Typical scanning electron micrographs of the fractured surfaces of $\text{Ca}(\text{OH})_2$ compacts prepared at (a) and (f) 1 MPa; (b) and (g) 3 MPa; (c) and (h) 5 MPa; (d) and (i) 10 MPa; (e) and (j) 15 MPa before carbonation (left column) and after carbonation for 72 h (right column). Bar: 5 μm

first several hours and a prolonged carbonation after 24 h gave only a slight increase in DTS values. Higher molding pressure resulted in a higher DTS value after 72 h of carbonation.

Figure 5 shows DTS values after carbonation for 72 h plotted against molding pressure. DTS values of the green compact before carbonation are also plotted in the figure. In both cases, we found that DTS values almost linearly increased with the molding pressure. Dependence of the DTS on molding pressure was much larger in the compact after carbonation, as shown in larger slope of the regression line. Thus the extent of increase in DTS by the carbonation became larger with the molding pressure.

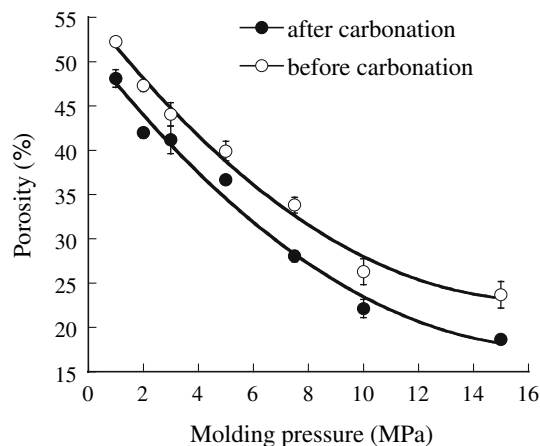


Fig. 3 Change in porosity of $\text{Ca}(\text{OH})_2$ compacts prepared at various molding pressures before and after carbonated for 72 h. The bars in the figure denote standard deviation

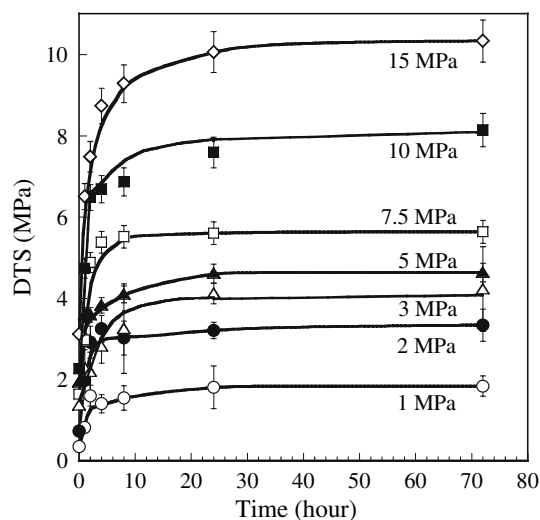


Fig. 4 Change in DTS values of $\text{Ca}(\text{OH})_2$ compacts prepared at various molding pressures as a function of carbonation time. The bars in the figure denote standard deviation

Discussion

The results obtained in the present study clearly demonstrated that $\text{Ca}(\text{OH})_2$ transformed directly to calcite, which is a most stable phase of calcium carbonate [11] when calcium hydroxide compacts were carbonated in CO_2 gas saturated with water vapor. The carbonation rate was almost the same irrespective of molding pressure and the carbonation almost completed within 72 h. At higher molding pressure, however, a small diffraction peak of $\text{Ca}(\text{OH})_2$ was still found at 2θ of 34.1° even after 72 h. Final conversion rate decreased from 99.8 wt% to 86.3 wt% with increasing in the molding pressure. This is probably caused by less penetration of CO_2 gas through

interparticles due to dense packing at higher molding pressure. In the other words, the Ca(OH)₂ compact prepared at higher molding pressure had less porosity, as shown in Fig. 3.

We also found that diffraction peaks of the calcite formed were broader than a commercially available calcite powder, which is well crystallized. Since the broadening of the diffraction peak is usually seen when the crystallite size became smaller, it is reasonable to consider that crystallite size of the calcite formed by the carbonation was smaller than the commercial one. As shown in Table 2, the crystallite size of the calcite obtained was between 35.2 nm and 46.8 nm and much smaller than that (83.4 nm) of the commercial calcite. The small crystallite size is preferable when the material is used as a bone substitute or a precursor of carbonate apatite preparation as a biomaterial.

During carbonation, no morphological changes was observed even at SEM level, it is probably due to the small crystallite size of calcite formed as already described. Therefore fine calcite crystals developed on the Ca(OH)₂ particles with keeping its original shape. As a matter of fact, the porosity was slightly decreased by about 4% before and after carbonation at each molding pressure. The decrease in porosity almost corresponds to a theoretical decrease of about 6% calculated under an assumption that a certain amount of Ca(OH)₂ compact transforms into calcite without changing its original volume. The carbonation proceeded by diffusion of CO₂ gas through the calcite layer initially formed on the original Ca(OH)₂ particle. Basically, smaller and less pores were observed in the Ca(OH)₂ compact prepared at higher molding pressure. This is also clearly demonstrated by change in porosity of Ca(OH)₂ compact after carbonation for 72 h with various molding pressure as shown in Fig. 3.

DTS rapidly increased in a first few hours and after that it gradually increased as shown in Fig. 4. The initial rapid increase is caused by the interparticle binding through calcite formed on the surface of the original Ca(OH)₂ particles. As already described, the extent of increase in DTS by the carbonation was larger at higher molding pressure, which was more effective for an intimate contact among the particles resulting in tight interparticle binding. As seen in Figs. 3 and 5, porosity decreases with molding pressure. This fact suggests that the final DTS mainly depends on the porosity. Actually, the following equation was theoretically derived to explain the relationship between the mechanical strength and porosity in brittle solid such as gypsum [12, 13]:

$$S = S_0 \log(P_{Cr}/P),$$

where S denotes mechanical strength and P denotes porosity. S₀ is a constant and P_{Cr} is defined as a critical

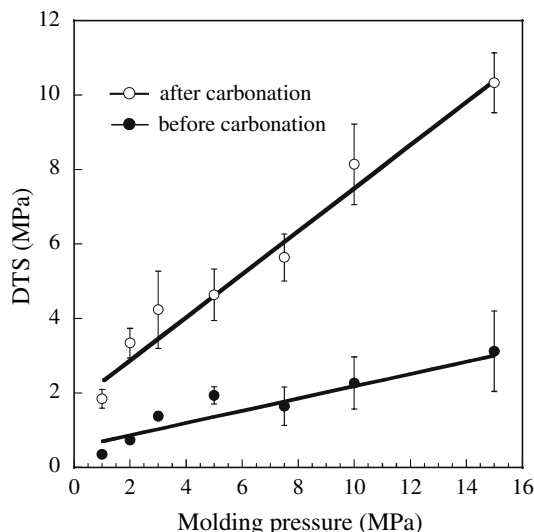


Fig. 5 DTS values before and after carbonation for 72 h plotted against molding pressure. The bars in the figure denote standard deviation

porosity, where the strength S becomes zero. Later, the equation was applied for the mechanical strength of dental gypsum [14] and biological calcium phosphate cement [15]. Figure 6 shows the relationship between DTS values and logarithm of porosity of specimens prepared at various molding pressures and those carbonated for 72 h. It was found that DTS values are inversely proportional to logarithm of porosity, that is, the above equation well holds. Critical porosity, P_{Cr} can be obtained by the extrapolation of the regression lines to zero of DTS. With the compact before and after the carbonation, P_{Cr} was 64.6% and

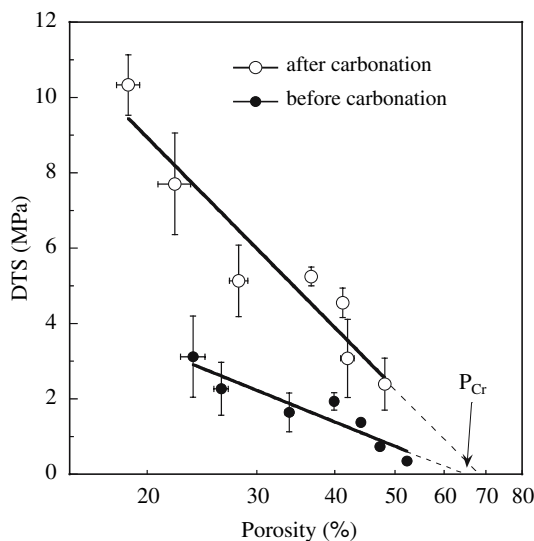


Fig. 6 The relation between DTS and logarithm of porosity of Ca(OH)₂ compacts before and after carbonation for 72 h. The bars in the figure denote standard deviation

68.4%, respectively, and both values almost coincided. This fact suggested that DTS values are determined by porosity in the calcite compact.

As shown in Fig. 5, specimens after carbonation for 72 h followed by being pressed at 1 MPa showed DTS values of 1.84 ± 0.25 MPa, and then linearly increased with the molding pressure, finally attained to 10.33 ± 0.80 MPa in the case of being pressed at 15 MPa, which is similar to that of set gypsum. The mechanical strengths are not sufficient for application to the areas exposed to large stress such as discontinuity defects of the jaw bones. However, it is enough for non load bearing area such as the holey bone defects caused by extirpation of tumors and cysts and the alveolar bone defects resulting from periodontal diseases. Moreover, when the calcite block is used as a bone substitute or as a precursor for the apatite like a coralline apatite, macroporosity plays an important role for penetration of cells and tissue fluid. Trial for fabrication of macroporus calcite block with higher porosity is now progress in our laboratory and a part of study will be published elsewhere [16].

Conclusion

For an artificial bone substitute, we prepared calcite compacts by carbonation of $\text{Ca}(\text{OH})_2$ compacts under various molding pressures ranged from 1 MPa to 15 MPa in CO_2 gas saturated with water vapor for various periods up to 72 h. It was found that $\text{Ca}(\text{OH})_2$ transformed directly to calcite and the transformation was not completed at higher molding pressure though its rate was almost the same irrespective of molding pressure. It was also found that DTS were determined by porosity in the calcite compact depending on molding pressure. There was a linear relation between DTS and logarithm of porosity.

This method enables us to obtain calcium carbonate compact with a wide range of mechanical strength by controlling the molding pressure.

Acknowledgments This study was supported in part by a Grant-in-aid for Scientific Research from the Ministry of Education, Sports, Culture, Science, and Technology, Japan.

References

1. F. SOUYRIS, C. PELLEQUER, C. PAYROT and C. SERVERA, *J. Maxillofac. Surg.* **13**(2) (1985) 64
2. G. GUILLEMIN, J. L. PATAT, J. FOURNIE and M. CHETAIL, *J. Biomed. Mater. Res.* **21**(5) (1987) 557
3. J. L. PATAT and G. GUILLEMIN, *Annal Chirurg Plast Esthet* **34**(3) (1989) 221
4. F. X. ROUX, D. BRASNU, B. LOTY, B. GEORGE and G. GUILLEMIN, *J. Neurosurg.* **69**(4) (1988) 510
5. F. X. ROUX, B. LOTY, D. BRASNU and G. GUILLEMIN, *Neuro-Chirurgie* **34**(2) (1988) 110
6. D. M. ROY and S. K. LINNEHAN, *Nature* **247** (1974) 220
7. M. SIVAKUMAR, T. S. KUMAR, K. L. SHANTHA and K. P. RAO, *Biomaterials* **17** (1996) 1709
8. W. SUCHANEK and M. YOSHIMURA, *J. Mater. Res.* **13** (1998) 94
9. J. C. FRICAIN, R. BAREILLE, F. ULYSSE, B. DUPUY and J. AMDEE, *J. Biomed. Mater. Res.* **42** (1998) 96
10. S. MATSUYA, X. LIN, K. UDOH, M. NAKAGAWA, R. SHIMOGORYO, Y. TERADA and K. ISHIKAWA, *J. Mater. Sci.: Mater. Med.* (2006) in press
11. L. N. PLUMMER and E. BUSENBERG, *Geochim Cosmochim Acta* **46** (1982) 1011
12. K. K. SCHILLER, in “Mechanical properties of non metallic brittle solids”, edited by W. H. Walton (Butterworth, London, 1958) p. 35
13. K. K. SHIHILLER, *Br. J. Appl. Phys.* **11** (1960) 338
14. T. MORI and M. YAMANE, *Aust. Dent. J.* **27**(1) (1982) 30
15. K. ISHIKAWA and K. ASAOKA, *J. Biomed. Mater. Res.* **29**(12) (1995) 1537
16. Y. LEE, Y. M. HAHM, S. MATSUYA, M. NAKAGAWA and K. ISHIKAWA, *J. Mater. Sci.* (2006) in press